Published in final edited form as:
Cancer Res. 2011 December 1; 71(23): 7291–7300. doi:10.1158/0008-5472.CAN-11-1715.

IKKβ and NFκB transcription govern lymphoma cell survival through AKT-induced plasma membrane trafficking of GLUT1

Thomas Sommermann[1], **Kathleen O'Neill**[1], **David R. Plas**[2], and **Ellen Cahir-McFarland**[1,3]

[1]The Department of Medicine, Division of Infectious Diseases, Brigham and Women's Hospital, Boston MA 02115

[2]The Department of Cancer and Cell Biology, University of Cincinnati, Cincinnati, OH 45267

Abstract

All cancer cells require increased nutrient uptake to support proliferation. Here we investigated the signals that govern glucose uptake in B-cell lymphomas and determined that the protein kinase IKKβ induced GLUT1 membrane trafficking in both viral and spontaneous B-cell lymphomas. IKKβ induced AKT activity, while IKKβ-driven NFκB transcription was required for GLUT1 surface localization downstream of AKT. Activated NFκB promoted AKT-mediated phosphorylation of the GLUT1 regulator, AKT Substrate 160kD (AS160), but was not required for AKT phosphorylation of the mammalian target of rapamycin (mTOR) regulator Tuberous Sclerosis 2 (TSC2). In Epstein Barr virus (EBV) transformed B-cells, NFκB inhibition repressed glucose uptake and induced caspase-independent cell death associated with autophagy. After NFκB inhibition, an alternate carbon source ameliorated both autophagy and cell death, whereas autophagy inhibitors specifically accelerated cell death. Taken together, the results suggest that NFκB signaling establishes a metabolic program supporting proliferation and apoptosis resistance by driving glucose import.

Introduction

Proto-oncogenes such as c-myc, Ras and PI3K or inactivation of tumor suppressors such as PTEN and p53 are associated with alterations in cellular metabolism commonly referred to as the Warburg effect (1). Glucose consumption, a hallmark of the Warburg effect (2–5), is shared by many B-lymphomas and most antigen or mitogen stimulated lymphocytes, suggesting the existence of a common regulatory mechanism to support rapid lymphocyte proliferation. NFκB activation is a common feature of transformed B lymphocytes such as Herpes virus transformed Lymphoblasts, multiple myeloma, Diffuse Large B Cell Lymphomas (DLBCL) and also mitogen stimulation or antigen co-receptor signaling in B-lymphocytes (6–9). For example Toll like Receptor (TLR) 4, TLR9, CD40 and BAFF-R engagement, as well as p53 depletion, were all shown to activate NFκB signaling and stimulate glucose consumption (10–12). We hypothesized that the NFκB pathway plays a critical role in glucose import.

NFκB transcription factors are latent in the cytoplasm until activated in response to upstream signals that converge upon the IKK complex composed of IKKγ, IKKα and IKKβ. IKKβ phosphorylates the Inhibitor of NFκB α (IκBα), thereby targeting it for proteasomal degradation, and allowing NFκB to translocate to the nucleus. Non-canonical stimuli

[3]Correspondance should be directed to Ellen Cahir-McFarland, 181 Longwood Ave, Boston, MA 02115, Phone: 617-525-4263, FAX: 617-525-4251, ecahir@rics.bwh.harvard.edu.

The authors declare no conflicts of interest.

activate IKKα to phosphorylate p100, induce p100 processing to p52 and its subsequent translocation to the nucleus (9). Some stimuli stabilize Bcl3 and its binding to p50 or p52 homodimers to turn these repressive complexes into transcriptional activators (13).

Glucose import across the cell membrane is mostly facilitated by Glucose transporters (GLUT) (14). GLUT levels and activity are highly regulated by oncogenes and tumor suppressors. c-myc and Ras induce GLUT1 mRNA (15, 16), whereas p53 suppresses GLUT1, 3 and 4 expression (12, 17). PI3K can induce GLUT1 and GLUT3 mRNA through HIF1α (18), but also induces translocation of GLUT4 from storage vesicles to the plasma membrane (14). PI3K induces GLUT4 trafficking by activating AKT that in turn phosphorylates AS160. AS160 phosphorylation inhibits its GTPase Activating Protein (GAP) function towards Rab proteins, which in their GTP bound form promote GLUT-vesicle movement to and fusion with the plasma membrane. Recently the PI3K AKT pathway was also implicated in the regulation of GLUT1 localization in T-cells (19, 20) Herein we investigate the effects of IKKβ and NFκB on glucose import and demonstrate that IKKβ and NFκB transcription govern B-lymphoblast survival through AKT-induced GLUT1 plasma membrane trafficking.

Materials and Methods

Cell culture

wtLCL23, a spontaneous LCL generated in the laboratory, and $IB4_{tet}$ΔNIκBα EBV+ LCLs (6), BL_{tet}LMP1 (21) and the DLBCLs SUDHL4 and 6 (22) were cultured in RPMI (GIBCO) supplemented with 2mM glutamine and 10% (v/v) Fetalplex (Gemini Bio-products). BC3, BCBL and BCML (KSHV+ PEL) (23–25) were cultured in RPMI supplemented with 2mM glutamine and 20% (v/v) Fetalplex. BL_{tet}LMP1 and $IB4_{tet}$ΔNIκBα were supplemented with 1μg/ml tetracycline, G418 (GIBCO;0.5mg/ml) and Hygromycin (EMD;1:1000). Cells harboring PGKop based vectors were cultured in Blasticidin (Invitrogen;1μg/ml). All cell lines were verified by viral gene expression and/or human CD19 expression and human CD54 expression. Cells were confirmed to be mycoplasma negative by MycoAlert (Lonza).

Vectors—PGKbla was created by ligating a Bgl2-EcoR1 encompassing the NFκB insensitive PGK promoter from PGK2 vector (26) into Bgl2-EcoR1 cut pcDNA6. PGKop was cloned by sequential ligation of EBNA1 as an AatII/MfeI and OriP as an Mfe1 fragments from pCEP4 into PGKbla cut with the same enzymes. EBNA1 and OriP, the EBV origin of replication, allow episomal maintenance of the plasmid. MyrAKT was cloned as a BamHI fragment from pBABEGFPmyrtAKT into PGKbla and PGKop. The AKT S473D mutation was introduced by quick change (Stratagene) with the oligonucleotide TTCCCCCAGTTCGACTACTCAGCTAGCGGCACAGCCTGA. GLUT1 with a 2xFlag tag in the first extracellular loop was provided by Jeff Rathmell (Duke University) (19) and cloned into PGKop as a Kpn1/Not1 fragment. As160 and AS160-4p (S318A, S588A, T642A, and S751A) vectors were provided by Gustav Lienhard (Dartmouth Medical School) (27). pN-2xHA-AS160 and pN-2xHA-AS160-4P were generated by amplifying coding sequences of AS160 and As160-4p with primers containing the recombination sites for Gateway cloning (forward primer: GGGGACAACTTTGTAC AAAAAAGTTGGCACCATGGAGCCGCCCAGCTGC; reverse primer: GGGGACAACTTTGTACAAGAAAGTTGGCAATGGCTTATTTCCTAT). PCR products were cloned into the pDONR223 gateway entry vector (Invitrogen) and shuttled into pN-2xHA. Vectors were introduced into IB4, $IB4_{tet}$ΔNIκBα and BL_{tet}LMP1 by AMAXA nucleofection (Solution V/Program X-05).

Cell culture manipulation

Unless noted, all chemical were purchased from SIGMA or EMD. 2-Amino-6-(2-(cyclopropylmethoxy)-6-hydroxyphenyl)-4-(4-piperidinyl)-3-pyridinecarbonitrile (IKKβi), and [5-(p-Fluorophenyl)-2-ureido]thiophene-3-carboxamide (IKKβi2), rapamycin, Q-VD-OPh Non-O-methylated, MG132, Wortmannin, LY294002 and oligomycin were dissolved in DMSO; Phloretin and tetracycline were dissolved in ethanol; LPS (Lipopolysaccharides Ecoli 026:B6), CpG (CpG Type B; Invivogen), choloroquine, 3-methyladenine (3MA), 10-(4′-(N-diethylamino)butyl)-2-chlorophenoxazin and cycloheximide (AKTi) were dissolved in water. Glutamine and α-ketoglutarate were dissolved in glucose free RPMI and the pH was adjusted to 7. To induce ΔNIκBα or LMP1 expression in $IB4_{tet}$ΔNIκBα and BL_{tet}LMP1, cells were washed three times with RPMI and cultured in RPMI with 10% tetracycline-approved serum (Clontech). For synthetic lethality assays, ΔNIκBα was induced for 48h and cells treated with indicated concentrations of Oligomycin, 3MA or Chloroquine for 16h. Cell survival was determined by FACS through propidium-iodide exclusion or shift in forward and side scatter. Cy5-AnnexinV (BD-Pharmingen) was used per the manufacturer.

Western Blot analysis

Cells were lysed on ice in RIPA buffer (50mM TRIS pH7.4, 150mM NaCl, 1mM EDTA, 1% NP-40, 0.5% DOC, 0.1% SDS, 1mM PMSF, 1% Protease inhibitor cocktail (Sigma), 2mM Na-pyrophosphate, 12.5mM β-glycerophosphate, 5mM NaF and1mM Na_3VO_4. Debris was pelleted at 10,000 rpm for 5mins. LC3B and GLUT1 samples were lysed in 60mM Tris pH 7.5 with 1% SDS at 100°C for 5min. The following antibodies were used in this study: from Santa Cruz Biotech, TRAF1, RELA, IRF3; from ABCAM, GLUT1, GLUT3, and AS160/TBC1d4; from Sigma, GAPDH, Tubulin, Flag M2&M5; from Cell Signaling, AKT, AKT pS473, pAKT T308, TSC2, TSC2 pT1462, S6K, S6K pT389, Pan AKT Substrate (PAS), LC3B, AMPKα, AMPKα pT172, HIF1α, P100/p52, RELA pS536; from Covance, HA-11. Tissue culture supernatants to LMP1 (mAB-S12) and c-myc (mAB-9E10) were used neat. Anti-mouse or rabbit secondary HRP antibodies were visualized using Western Lightning Plus chemiluminescent substrate (Pierce) and a Kodak Image Station 4000R.

Surface GLUT1 assays

Cells were stained for 20min at 4°C with a polyclonal rabbit anti-Flag antibody (1:200, Sigma) in FACS buffer (PBS, 0.1% SoAzide and 5% serum). Cells were washed and labeled with Alexa Fluor conjugated antibodies 1:200 in FACS buffer for 20min at 4°C. Median fluorescence intensity of live cells (FSC/SSC gating) was determined by FACS and, if indicated, normalized to fGLUT1 over GAPDH expression. For transient assays expression vectors were cotransfected with peGFP-C1 (Clontech) and surface fGLUT1 levels was determined on GFP+ cells.

2-NBDG uptake

(2-(N-(7-nitrobenz-2-oxa-1,3-diazol-4-yl)amino)-2-deoxyglucose) 2NBDG, a glucose analogue fluorescently labeled at the 2 position, is a substrate for glucose transporters, independent of metabolic reactions downstream of Hexokinase (28). Cells were brought up in RPMI 10% serum and 50μM 2-NBDG. Median cell fluorescence was measured at multiple time points between 5 and 32min. The increase in fluorescence was linear and inhibited at 4°C. The slope of a linear regression was defined as the rate of glucose uptake and normalized to the rate of 2NBDG uptake of corresponding control cells. When indicated, Phloretin (250μM) was included 15min prior to and during the assay.

Lactate assay

Cells were washed 3x and cultured for 4h in RPMI with 10% dialyzed serum (dialyzed 2x, with MWCO 3500Da, against 100x volume of PBS, 24h). Lactate in the cell supernatants were measured with a lactate assay (Biovision) per the manufactures instructions and normalized to cell concentration.

Immunofluorescence

Concentrated cells were transferred in RPMI onto Poly-D-lysine coated coverslips for 15min, fixed with 50% Methanol 50% Acetone for 2min, blocked with RPMI/10% serum for 30min, and incubated in primary antibody in RPMI/10% serum overnight. Cells were washed, incubated with species specific Alexa Flour conjugated antibodies and TO-PRO3 DNA stain (1:400;Invitrogen). Slides were mounted with ProLong Antifade solution (Invitrogen) and imaged with a Nikon PCM2000 coupled to Zeiss inverted fluorescence microscope using Simple 32 software. GLUT1, GLUT3, HA and LC3 brightness was individually adjusted in Adobe Photoshop for maximal brightness. All LMP1 images in a single panel were acquired with the same exposure time and the brightness was adjusted identically. Nuclei staining (brightness and gamma) was corrected for optimal visualization.

Immunoprecipitation

Cells were lysed for 20min in ice cold IP buffer (20mM Tris pH7.5, 50mM NaCl,1mM EDTA, 1% NP40, 2.5mM Na pyrophosphate, 1mM β-glycerophosphate, 1mM Na_3VO_4, 1% protease inhibitor cocktail (Sigma), 1mM PMSF). AS160 was immunoprecipitated with 1μg anti-AS160 antibody and 20μl sepharose A beads (Invitrogen) rotating at 4°C for 4h from cleared supernatants (10,000rpm for 5min).

Statistical analysis

Statistical differences were determined with a two-tailed paired Student's t-test. P-values are indicated.

Results

IKKβ induces GLUT dependent Glucose import

To examine glucose import, we monitored uptake of a fluorescent 2-deoxyglucose analog (2NBDG) (28) in response to signals from the NFκB activators Epstein-Barr Virus (EBV) oncoprotein Latent Membrane Protein 1 (LMP1), LPS or CpG, in the $NF\kappa B^{low}$ Burkitt's lymphoma cell line BL41 that was stably transfected with LMP1 under tetracycline control (BLtetLMP1). All stimuli independently increased the rate of glucose uptake (Figure 1A), but failed to do so in the presence of chemical IKKβ inhibitors (IKKβi or IKKβi2) that specifically blocked canonical signaling (Figure 1A, S1A, S1B). Supernatant transfer from LMP1+ to LMP1- cells did not induce glucose import to the same extent indicating that NFκB regulation of glucose import is cell intrinsic and not due to elevated cytokine secretion (Figure S1C). Phloretin, a specific GLUT inhibitor, blocked LMP1-induced glucose import (Figure S1D) indicating that LMP1-mediated NFκB effects were dependent on GLUT family proteins. Therefore, we evaluated expression levels and localization of the predominant lymphoid GLUT family members, GLUT1 and GLUT3 (21, 29). LMP1 and LPS induced the NFκB target TRAF1, and IKKβi prevented TRAF1 induction (Figures 1B, 1C). Perturbation of the NFκB pathway had no impact on GLUT1, GLUT3, or their transcriptional regulators HIF1α or c-myc, (15, 18) (Figures 1B, 1C, S1E).

IKKβ induces GLUT1 membrane localization

Although GLUT abundance was not affected by IKKβ activation, we observed clear regulation of GLUT1 localization. In response to EBV LMP1, LPS and CpG GLUT1 translocated from intracellular vesicles to the plasma membrane (Figure 1D). In contrast, GLUT3 localized to cytosolic punctae independent of LMP1 expression (Figure S1F). In agreement with the glucose import assays, IKKβi blocked the ability of all three independent stimuli to promote GLUT1 plasma membrane localization (Figure 1D). To quantify the impact of IKKβ inactivation on GLUT1 plasma membrane levels, we stably expressed GLUT1 modified with a 2x Flag tag (fGLUT1) in the first extracellular loop (19) in BLtetLMP1 (BLtetLMP1-fGLUT1). LMP1 and LPS significantly increased surface fGLUT1 (Figure S1G-K) independent of fGLUT1 expression levels (Figure S1K-M). This effect was dependent on IKKβ activity (Figure S1H-M). Further, IKKβi caused GLUT1 retention in wild type lymphoblastoid cell lines (LCLs), Kaposi's Sarcoma Herpes Virus (KSHV) infected Peripheral Effusion Lymphomas (PEL) and DLBCL, demonstrating that IKKβ governs GLUT1 localization in many B-cell malignancies (Figure 1E,S1N).

IKKβ and PI3K are required for AKT activation

GLUT1 plasma membrane localization in lymphocytes is regulated in a manner similar to GLUT4 in adipocytes, where GLUT4 translocates to the plasma membrane in response to insulin induced PI3K and AKT activation (14, 19). Therefore, we sought to determine if GLUT1 trafficking in response to NFκB stimuli is AKT dependent. Like IKKβ inhibitors, the PI3K inhibitor LY294002 prevented LMP1-, LPS-, and CpG-induced GLUT1 translocation and glucose import (Figure 2A, 2B). Futher, PI3K inhibition by Wortmannin and LY294002 or AKT inhibition by an AKT inhibitor (AKTi) led to retention of endogenous GLUT1 in wtLCL23, BCML and SUDHL4 lymphoma cells and fGLUT1 in IB4-fGLUT1 (Figure S2A-D). These data indicate that GLUT1 localization is PI3K, AKT and IKKβ dependent. As LMP1 and TLRs can activate AKT (30–32) we sought to determine if IKKβ functions in the AKT pathway. Indeed, both PI3K and IKKβ inhibitors blocked LMP1- and LPS-induced AKT activation (Figure 2C, 2D). In fact, IKKβi reduced LMP1-induced AKT activity within 5 hours (Figure S2E). In contrast to LMP1 and LPS, serum-induced AKT activation was unaffected by IKKβi (Figure S2F) indicating that the role of IKKβ does not extend to growth factor receptors and demonstrating the specificity of the IKKβ inhibitor. The IKKβ related TANK-binding kinase 1 (TBK1) was shown to phosphorylate AKT at S473 (33) raising the possibility that IKKβi effects may be mediate by TBK1 inhibition. However, IKKβi specifically inhibited Sendai virus-induced IKKβ-dependent RelA S536 phosphorylation with no effect on TBK1-dependent IRF3 dimerization (Figure S2G) (34) and neither LMP1, nor LPS, induced IRF3 dimerization in BLtetLMP1 (Figure S2H).

Since IKKβi caused GLUT1 retention in wtLCLs23, BCLM and SUDHL4, we examined the effect of IKKβi on AKT activity in these cell lines. IKKβi only modestly reduced AKT S473 phosphorylation (Figure S2C), suggesting that IKKβ had a second effect on GLUT1 trafficking. This was supported by the observation that CHX had no effect on LPS-induced AKT activation (Figure 2D), but completely blocked LPS- or CpG- induced surface GLUT1 translocation and glucose import (Figure 2A,2B,S1J). Thus, IKKβ induces AKT that in turn is essential for GLUT1 plasma membrane accumulation. Yet AKT activation is not sufficient for GLUT1 plasma membrane targeting in the absence of continuous protein synthesis. We reasoned that NFκB- or AKT-mediated gene expression may be necessary for IKKβ stimuli to promote AKT-regulated GLUT1 localization.

NFκB transcription supports GLUT1 membrane localization downstream of AKT

To determine the requirement for NFκB transcription on GLUT1 localization and glucose import, NFκB complexes were retained in the cytoplasm by a tetracycline-inducible NFκB superrepressor, ΔNIκBα, in the LMP1+ lymphoblastoid cell line IB4 ($IB4_{tet}$ΔNIκBα) (11). NFκB inhibition caused a loss of glucose import and surface endogenous- or flag-GLUT1 over three days (Figure 3A,3B,S3A,S3B,S1G) without impacting GLUT1 and 3 expression or GLUT3 localization (Figure 3C,S1F). ΔNIκBα modestly decreased AKT S473 phosphorylation without impacting AKT phosphorylation at the PDK1 site T308 or its activity towards an established target, TSC2 (Figure S3C) (35). To test NFκB transcriptional effects on GLUT1 localization independent of AKT regulation, we expressed constitutively active myristoylated AKT (myrAKT) and myrAKT with a S473D mutation (myrAKTS473D) in $IB4_{tet}$ΔNIκBα and $IB4_{tet}$ΔNIκBα-fGLUT1. The activating S473D mutation renders AKT activity independent of S473 phosphorylation (36). myrAKT and myrAKTS473D sustained surface endogenous- or flag-GLUT1 levels after Wortmannin treatment, but failed to do so after inhibition of NFκB transcription (Figure 3D, 3E). Similarly, glucose import in myrAKT and myrAKTS473D expressing cells was elevated over control cells but still dependent on NFκB-mediated transcription (Figure S3D). Note that myrAKT and myrAKTS473D expression levels were not altered (Figure S3E). As constitutive AKT signaling did not overcome the effects of ΔNIκBα, NFκB-mediated gene expression is required for surface localization of GLUT1 downstream or independent of AKT activity.

NFκB transcription is essential for AKT-mediated AS160 phosphorylation

AKT promotes GLUT4 membrane localization by inhibitory phosphorylation of AKT Substrate of 160kDa (AS160) (14). To analyze AS160 impact on GLUT1 localization in lymphocytes, we transfected IB4 or IB4ΔNIκBα-fGLUT1 with expression vectors for either control, HA-AS160 or mutant HA-AS160 lacking all AKT phosphorylation sites (HA-AS160-4p; S318A, S588A, T642A, and S751A) (27). HA-AS160 expression had no impact on GLUT1 localization, while HA-AS160-4p caused retention of both endogenous-and fGLUT1 (Figure 4A, 4B).Thus AS160 is an essential regulator of GLUT1 membrane localization in B-lymphocytes. Consistent with constitutive GLUT1 localization at the plasma membrane, AS160 was phosphorylated at AKT sites (pan AKT substrate, PAS) in $IB4_{tet}$ΔNIκBα (Figure 4C). Wortmannin inhibited AS160 PAS-phosphorylation in control uninduced cells, but had little effect in $IB4_{tet}$ΔNIκBα stably expressing myrAKT or myrAKTS473D (Figure 4C).

Rapamycin blocked TORC1-dependent phosphorylation of S6K at T389 but had no impact on AS160 phosphorylation and very little effect on surface endogenous- or flag-GLUT1 (Figure 4C, S3F, S2B).

We discovered that NFκB is specifically required to recruit AKT for the phosphorylation of AS160. Inhibition of NFκB-mediated transcription by ΔNIκBα resulted in loss of AS160 PAS site phosphorylation in control, myrAKT and myrAKT S473D expressing cells (Figure 4D). Importantly, the effect of NFκB was specific to AS160 as AKT target TSC2 T1462 phosphorylation was unaffected by NFκB inhibition (Figure 4D). Moreover the activity of AMPKα, which can promote AS160 phosphorylation (21), was not altered after NFκB inhibition (Figure S1E). Thus, we have shown that the NFκB pathway has two roles in GLUT1 localization. IKKβ is required for AKT activation, whereas NFκB-mediated transcription allows AKT to phosphorylate AS160 (Figure 4E).

Carbon availability is a significant feature of NFκB pro survival signaling

To assess the importance of NFκB effects on GLUT1 and lymphoma cell metabolism, we used EBV transformed lymphoblastoid cells. EBV transforms primary B cells into lymphoblastoid cells, without somatic mutations, that are highly reliant on EBV LMP1-mediated NFκB activation for proliferation and survival (6). LCLs die after NFκB inhibition over the course of one week and cell death is not abrogated by caspase inhibitors ((6) and Figure S4A). Since ΔNIκBα reduced glucose import resulting in decreased lactate secretion (Figure 5A), we determined if reduced carbon availability contributed to LCL cell death after NFκB inhibition. NFκB inhibited cells were cultured with additional substrates for the TCA-cycle. Increasing the initial glutamine concentration from 2 to 22mM and adding 20mM α-ketoglutarate improved $IB4_{tet}$ΔNIκBα survival from 40% to 59% five days after ΔNIκBα expression (Figure 5B). Further, NFκB inhibition increased sensitivity to the respiratory chain inhibitor oligomycin even in the presence of caspase inhibitor QVD, indicating that NFκB inhibition renders LCLs more reliant on mitochondrial metabolism (Figure S4B, S4C). Macro autophagy (here autophagy) can be induced as a pro survival mechanism during starvation to sustain ATP and carbon availability by degrading cytosolic components (37). As has been observed in other LCLs (38), uninduced $IB4_{tet}$ΔNIκbα exhibited low levels of autophagy as measured by LC3b foci (Figure 5C). Three days afterΔNIκBα induction, we observed a dramatic accumulation of LC3b foci (Figure 5C) and of autophagosome-associated, phosphatidylethanolamine-conjugated, LC3b (LC3b II) in the corresponding cell lysates (Figure 5D). Both indicators of autophagy were reduced when cells were grown in high glutamine and α-ketoglutarate indicating that ΔNIκBα caused starvation that in turn induced autophagy (Figure 5C, 5D). Interestingly, the autophagy inhibitors 3-methyladenine (Figure 5E) or chloroquine (Figure S4D) accelerated LCL death in NFκB inhibited cells but had no effect on NFκB active cells. Glutamine and α-ketoglutarate partially reversed the increased sensitivity to autophagy inhibitors (Figure 5E, S4D).

Discussion

To support macromolecule synthesis, proliferating cells need to elevate nutrient uptake. B-cells utilize glucose as their predominant carbon source. Herein, we have provided novel evidence that the IKKβ/NFκB pathway induces glucose import by supporting GLUT1 plasma membrane localization. IKKβ kinase activity and NFκB transcription function by regulating GLUT1 trafficking at separate points in the AKT pathway (Figure 4E). Further, we show that stimulation of glucose transport is a significant feature of NFκB prosurvival signaling. IKKβ and PI3K activity are necessary for LMP1 and LPS to stimulate AKT. AKT also activates the IKK complex (39) creating a feed forward mechanism that potentiates AKT activity. Recently, the IKKβ related kinase, TBK1, was shown to phosphorylate AKT at S473 (33), raising the possibility that IKKβ might directly phosphorylate AKT. However, IKKβ may phosphorylate any of the numerous proteins that are established modifiers of PI3K dependent AKT activation.

The requirement for IKKβ in LMP1- and LPS-mediated AKT activation and GLUT1 plasma membrane localization contrasts with the effect of TNFα-mediated IKKβ activity on GLUT4 trafficking (40). In adipocytes TNFα inhibits insulin induced GLUT4 membrane translocation through IKKβ-mediated inhibitory phosphorylation of IRS1 at S312. This divergent role for IKKβ may arise from stimulus dependent differences in IKKβ complex formation. TNFR1 activates IKKβ via RIP1 whereas LMP1 and TLRs activate IKKβ via TRAF6 (41–43). Potentially only RIP1-IKKβ complexes recruit and phosphorylate IRS1, whereas TRAF6-IKKβ complexes do not. Consistent with this idea, we could not detect IRS1 phosphorylation at S312 despite constitutive IKKβ activity in Lymphoblastoid cell lines (data not shown).

In contrast to IKKβ kinase activity, NFκB-mediated transcription modulated AKT substrate recognition. Nuclear translocation of NFκB subunits is essential for AKT phosphorylation of AS160, but not TSC2. Thus NFκB inhibition uncouples AKT effects on glucose import from mTORC1 activation and illustrates a novel way of stimulus dependent AKT substrate recognition. Although the identity of the transcriptional target(s) is unknown, we favor a simple model in which NFκB drives transcription of a gene encoding a scaffold that allows AKT to interact with AS160. It is possible that such a scaffold also regulates additional AKT substrate recognition. Our results parallel the requirement for NFκB and AKT in LMP1 induced migration in nasopharyngeal carcinomas and LMP1-induced lymphoma in transgenic mice (31, 44).

Tumor viruses like EBV and KSHV evolved to exploit the normal signaling pathways that drive lymphocyte proliferation. Here, we have shown that EBV oncogene LMP1 and TLRs use the same IKKβ- and AKT-dependent mechanisms to stimulate glucose import. The importance of NFκB-stimulated glucose import is evident as glutamine and α-ketoglutarate ameliorated the effects of NFκB inhibition including autophagosome formation, the dependence on autophagy, and cell death. These data support a model where NFκB promotes survival of NFκB dependent lymphomas by ensuring ample glucose import for energy production and macromolecule synthesis. Autophagy is triggered through starvation after NFκB inhibition to prolong survival by providing alternative substrates for metabolism (Figure 5F).

It is not clear why 2mM glutamine (media concentration) was not sufficient to saturate glutamine metabolism. Recently, Wellen and colleagues have shown that hexosamines, predominantly derived from imported glucose, are necessary to transport glutamine (45). The supplementation of 22mM glutamine and 20mM α-ketoglutarate might be required to overcome decreased glutamine import secondary to decreased glucose import after NFκB inhibition.

NFκB inhibition sensitized lymphoblastoid cells to inhibitors of oxidative phosphorylation or autophagy. The combined targeting of NFκB-mediated transcription and autophagy or mitochondrial metabolism is likely to be a highly effective chemotherapeutic strategy for lymphoma. NFκB transcription has also been shown to be essential in colorectal, breast, and lung cancer, but generally thought to do so through induced expression of antiapoptotic proteins (46, 47). Yet, many of these tumors have high GLUT1 expression (48, 49), which is important for cell survival and associated with poor clinical prognosis (16, 50). Therefore, NFκB may also contribute to enhanced survival in these tumors by facilitating AKT substrate interactions, GLUT1 membrane targeting and glucose import.

Supplementary Material

Refer to Web version on PubMed Central for supplementary material.

Acknowledgments

We are grateful to Micah Luftig, Daniela Boehm, Benjamin Gewurz, Brendan Manning, Bruce Horwitz, and Elliott Kieff for helpful discussions, to Jeff Rathmell for the Flag-GLUT1 cDNA, to Takahiro Nagase and Gustav Lienhard for the KIAA0603/AS160 constructs, and to Michaela Gack for the Sendai virus and her assistance with the native page. T.S. was a GSK fellow 2008 and is member of the Graduate College “Viruses of the Immune System” at the University of Erlangen-Nurnberg. This work was supported by NIH PHS grant CA085180.

This work was supported by NIH PHS grant CA085180.

References

1. Vander Heiden MG, Cantley LC, Thompson CB. Understanding the Warburg effect: the metabolic requirements of cell proliferation. Science. 2009; 324:1029–33. [PubMed: 19460998]
2. Wang T, Marquardt C, Foker J. Aerobic glycolysis during lymphocyte proliferation. Nature. 1976; 261:702–5. [PubMed: 934318]
3. Sariban-Sohraby S, Magrath IT, Balaban RS. Comparison of energy metabolism in human normal and neoplastic (Burkitt's lymphoma) lymphoid cells. Cancer Res. 1983; 43:4662–4. [PubMed: 6883323]
4. Elstrom R, Guan L, Baker G, Nakhoda K, Vergilio JA, Zhuang H, et al. Utility of FDG-PET scanning in lymphoma by WHO classification. Blood. 2003; 101:3875–6. [PubMed: 12531812]
5. Jacobs SR, Herman CE, Maciver NJ, Wofford JA, Wieman HL, Hammen JJ, et al. Glucose uptake is limiting in T cell activation and requires CD28-mediated Akt-dependent and independent pathways. J Immunol. 2008; 180:4476–86. [PubMed: 18354169]
6. Cahir-McFarland ED, Davidson DM, Schauer SL, Duong J, Kieff E. NF-kappa B inhibition causes spontaneous apoptosis in Epstein-Barr virus-transformed lymphoblastoid cells. Proc Natl Acad Sci U S A. 2000; 97:6055–60. [PubMed: 10811897]
7. Li ZW, Chen H, Campbell RA, Bonavida B, Berenson JR. NF-kappaB in the pathogenesis and treatment of multiple myeloma. Curr Opin Hematol. 2008; 15:391–9. [PubMed: 18536579]
8. Davis RE, Brown KD, Siebenlist U, Staudt LM. Constitutive nuclear factor kappaB activity is required for survival of activated B cell-like diffuse large B cell lymphoma cells. J Exp Med. 2001; 194:1861–74. [PubMed: 11748286]
9. Perkins ND, Gilmore TD. Good cop, bad cop: the different faces of NF-kappaB. Cell Death Differ. 2006; 13:759–72. [PubMed: 16410803]
10. Krawczyk CM, Holowka T, Sun J, Blagih J, Amiel E, DeBerardinis RJ, et al. Toll-like receptor-induced changes in glycolytic metabolism regulate dendritic cell activation. Blood. 2010; 115:4742–9. [PubMed: 20351312]
11. Woodland RT, Fox CJ, Schmidt MR, Hammerman PS, Opferman JT, Korsmeyer SJ, et al. Multiple signaling pathways promote B lymphocyte stimulator dependent B-cell growth and survival. Blood. 2008; 111:750–60. [PubMed: 17942753]
12. Kawauchi K, Araki K, Tobiume K, Tanaka N. p53 regulates glucose metabolism through an IKK-NF-kappaB pathway and inhibits cell transformation. Nat Cell Biol. 2008; 10:611–8. [PubMed: 18391940]
13. Thornburg NJ, Pathmanathan R, Raab-Traub N. Activation of nuclear factor-kappaB p50 homodimer/Bcl-3 complexes in nasopharyngeal carcinoma. Cancer Res. 2003; 63:8293–301. [PubMed: 14678988]
14. Zaid H, Antonescu CN, Randhawa VK, Klip A. Insulin action on glucose transporters through molecular switches, tracks and tethers. Biochem J. 2008; 413:201–15. [PubMed: 18570632]
15. Osthus RC, Shim H, Kim S, Li Q, Reddy R, Mukherjee M, et al. Deregulation of glucose transporter 1 and glycolytic gene expression by c-Myc. J Biol Chem. 2000; 275:21797–800. [PubMed: 10823814]
16. Yun J, Rago C, Cheong I, Pagliarini R, Angenendt P, Rajagopalan H, et al. Glucose deprivation contributes to the development of KRAS pathway mutations in tumor cells. Science. 2009; 325:1555–9. [PubMed: 19661383]
17. Schwartzenberg-Bar-Yoseph F, Armoni M, Karnieli E. The tumor suppressor p53 down-regulates glucose transporters GLUT1 and GLUT4 gene expression. Cancer Res. 2004; 64:2627–33. [PubMed: 15059920]
18. Zelzer E, Levy Y, Kahana C, Shilo BZ, Rubinstein M, Cohen B. Insulin induces transcription of target genes through the hypoxia-inducible factor HIF-1alpha/ARNT. Embo J. 1998; 17:5085–94. [PubMed: 9724644]
19. Wieman HL, Wofford JA, Rathmell JC. Cytokine stimulation promotes glucose uptake via phosphatidylinositol-3 kinase/Akt regulation of Glut1 activity and trafficking. Mol Biol Cell. 2007; 18:1437–46. [PubMed: 17301289]

20. Wofford JA, Wieman HL, Jacobs SR, Zhao Y, Rathmell JC. IL-7 promotes Glut1 trafficking and glucose uptake via STAT5-mediated activation of Akt to support T-cell survival. Blood. 2008; 111:2101–11. [PubMed: 18042802]
21. Cahir-McFarland ED, Carter K, Rosenwald A, Giltnane JM, Henrickson SE, Staudt LM, et al. Role of NF-kappa B in cell survival and transcription of latent membrane protein 1-expressing or Epstein-Barr virus latency III-infected cells. J Virol. 2004; 78:4108–19. [PubMed: 15047827]
22. Yecies D, Carlson NE, Deng J, Letai A. Acquired resistance to ABT-737 in lymphoma cells that up-regulate MCL-1 and BFL-1. Blood. 2010; 115:3304–13. [PubMed: 20197552]
23. Arvanitakis L, Mesri EA, Nador RG, Said JW, Asch AS, Knowles DM, et al. Establishment and characterization of a primary effusion (body cavity-based) lymphoma cell line (BC-3) harboring kaposi's sarcoma-associated herpesvirus (KSHV/HHV-8) in the absence of Epstein-Barr virus. Blood. 1996; 88:2648–54. [PubMed: 8839859]
24. You J, Srinivasan V, Denis GV, Harrington WJ Jr, Ballestas ME, Kaye KM, et al. Kaposi's sarcoma-associated herpesvirus latency-associated nuclear antigen interacts with bromodomain protein Brd4 on host mitotic chromosomes. J Virol. 2006; 80:8909–19. [PubMed: 16940503]
25. Renne R, Zhong W, Herndier B, McGrath M, Abbey N, Kedes D, et al. Lytic growth of Kaposi's sarcoma-associated herpesvirus (human herpesvirus 8) in culture. Nat Med. 1996; 2:342–6. [PubMed: 8612236]
26. Boehm D, Gewurz BE, Kieff E, Cahir-McFarland E. Epstein-Barr latent membrane protein 1 transformation site 2 activates NF-kappaB in the absence of NF-kappaB essential modifier residues 133–224 or 373–419. Proc Natl Acad Sci U S A. 2010; 107:18103–8. [PubMed: 20923877]
27. Sano H, Kane S, Sano E, Miinea CP, Asara JM, Lane WS, et al. Insulin-stimulated phosphorylation of a Rab GTPase-activating protein regulates GLUT4 translocation. J Biol Chem. 2003; 278:14599–602. [PubMed: 12637568]
28. O'Neil RG, Wu L, Mullani N. Uptake of a fluorescent deoxyglucose analog (2-NBDG) in tumor cells. Mol Imaging Biol. 2005; 7:388–92. [PubMed: 16284704]
29. Rathmell JC, Vander Heiden MG, Harris MH, Frauwirth KA, Thompson CB. In the absence of extrinsic signals, nutrient utilization by lymphocytes is insufficient to maintain either cell size or viability. Mol Cell. 2000; 6:683–92. [PubMed: 11030347]
30. Herrera-Velit P, Reiner NE. Bacterial lipopolysaccharide induces the association and coordinate activation of p53/56lyn and phosphatidylinositol 3-kinase in human monocytes. J Immunol. 1996; 156:1157–65. [PubMed: 8557993]
31. Shair KH, Bendt KM, Edwards RH, Bedford EC, Nielsen JN, Raab-Traub N. EBV latent membrane protein 1 activates Akt, NFkappaB, and Stat3 in B cell lymphomas. PLoS Pathog. 2007; 3:e166. [PubMed: 17997602]
32. Dawson CW, Tramountanis G, Eliopoulos AG, Young LS. Epstein-Barr virus latent membrane protein 1 (LMP1) activates the phosphatidylinositol 3-kinase/Akt pathway to promote cell survival and induce actin filament remodeling. J Biol Chem. 2003; 278:3694–704. [PubMed: 12446712]
33. Ou YH, Torres M, Ram R, Formstecher E, Roland C, Cheng T, et al. TBK1 directly engages Akt/PKB survival signaling to support oncogenic transformation. Mol Cell. 2011; 41:458–70. [PubMed: 21329883]
34. Fitzgerald KA, McWhirter SM, Faia KL, Rowe DC, Latz E, Golenbock DT, et al. IKKepsilon and TBK1 are essential components of the IRF3 signaling pathway. Nat Immunol. 2003; 4:491–6. [PubMed: 12692549]
35. Laplante M, Sabatini DM. mTOR signaling at a glance. J Cell Sci. 2009; 122:3589–94. [PubMed: 19812304]
36. Alessi DR, Andjelkovic M, Caudwell B, Cron P, Morrice N, Cohen P, et al. Mechanism of activation of protein kinase B by insulin and IGF-1. Embo J. 1996; 15:6541–51. [PubMed: 8978681]
37. Degenhardt K, Mathew R, Beaudoin B, Bray K, Anderson D, Chen G, et al. Autophagy promotes tumor cell survival and restricts necrosis, inflammation, and tumorigenesis. Cancer Cell. 2006; 10:51–64. [PubMed: 16843265]

38. Paludan C, Schmid D, Landthaler M, Vockerodt M, Kube D, Tuschl T, et al. Endogenous MHC class II processing of a viral nuclear antigen after autophagy. Science. 2005; 307:593–6. [PubMed: 15591165]
39. Romashkova JA, Makarov SS. NF-kappaB is a target of AKT in anti-apoptotic PDGF signalling. Nature. 1999; 401:86–90. [PubMed: 10485711]
40. Nieto-Vazquez I, Fernandez-Veledo S, Kramer DK, Vila-Bedmar R, Garcia-Guerra L, Lorenzo M. Insulin resistance associated to obesity: the link TNF-alpha. Arch Physiol Biochem. 2008; 114:183–94. [PubMed: 18629684]
41. Lomaga MA, Yeh WC, Sarosi I, Duncan GS, Furlonger C, Ho A, et al. TRAF6 deficiency results in osteopetrosis and defective interleukin-1, CD40, and LPS signaling. Genes Dev. 1999; 13:1015–24. [PubMed: 10215628]
42. Schultheiss U, Puschner S, Kremmer E, Mak TW, Engelmann H, Hammerschmidt W, et al. TRAF6 is a critical mediator of signal transduction by the viral oncogene latent membrane protein 1. Embo J. 2001; 20:5678–91. [PubMed: 11598011]
43. Ting AT, Pimentel-Muinos FX, Seed B. RIP mediates tumor necrosis factor receptor 1 activation of NF-kappaB but not Fas/APO-1-initiated apoptosis. Embo J. 1996; 15:6189–96. [PubMed: 8947041]
44. Shair KH, Schnegg CI, Raab-Traub N. EBV latent membrane protein 1 effects on plakoglobin, cell growth, and migration. Cancer Res. 2008; 68:6997–7005. [PubMed: 18757414]
45. Wellen KE, Lu C, Mancuso A, Lemons JM, Ryczko M, Dennis JW, et al. The hexosamine biosynthetic pathway couples growth factor-induced glutamine uptake to glucose metabolism. Genes Dev. 2010; 24:2784–99. [PubMed: 21106670]
46. Karin M. Nuclear factor-kappaB in cancer development and progression. Nature. 2006; 441:431–6. [PubMed: 16724054]
47. Meylan E, Dooley AL, Feldser DM, Shen L, Turk E, Ouyang C, et al. Requirement for NF-kappaB signalling in a mouse model of lung adenocarcinoma. Nature. 2009; 462:104–7. [PubMed: 19847165]
48. Godoy A, Ulloa V, Rodriguez F, Reinicke K, Yanez AJ, Garcia Mde L, et al. Differential subcellular distribution of glucose transporters GLUT1-6 and GLUT9 in human cancer: ultrastructural localization of GLUT1 and GLUT5 in breast tumor tissues. J Cell Physiol. 2006; 207:614–27. [PubMed: 16523487]
49. Ozbudak IH, Shilo K, Tavora F, Rassaei N, Chu WS, Fukuoka J, et al. Glucose transporter-1 in pulmonary neuroendocrine carcinomas: expression and survival analysis. Mod Pathol. 2009; 22:633–8. [PubMed: 19234439]
50. Haber RS, Rathan A, Weiser KR, Pritsker A, Itzkowitz SH, Bodian C, et al. GLUT1 glucose transporter expression in colorectal carcinoma: a marker for poor prognosis. Cancer. 1998; 83:34–40. [PubMed: 9655290]

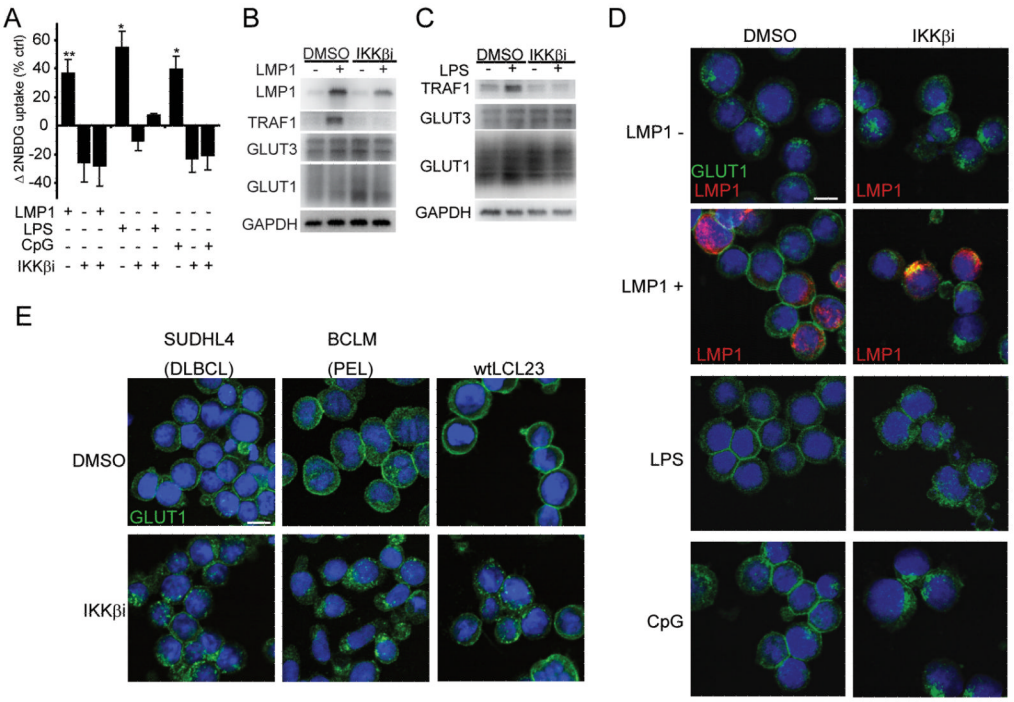

Figure 1. EBV LMP1-, LPS- and CpG- stimulate glucose import and promote GLUT1 plasma membrane localization via IKKβ

(A) Glucose uptake was measured by 2NBDG fluorescence in BLtetLMP1 induced to express LMP1 (24h), stimulated with LPS (500ng/ml;10h), or stimulated with CpG (250nM; 10h). IKKβi (10μM) or DMSO were included at 9h (LMP1) or 0h (LPS/CpG). Percent change of 2NBDG uptake over control cells is presented (n=4 LMP1; n=3 LPS/CpG; mean ±s.d., *p<0.05 /** p<0.005) **(B and C)** GLUT1 and GLUT3 expression in total cell lysates from (A). TRAF1 and GAPDH expression serves as controls for NFκB activity and protein content. **(D)** GLUT1 (green), DNA (blue), and where indicated, LMP1 (red) immunofluorescence of cells from (A). **(E)** GLUT1 localization in IKKβi or DMSO treated SUDHL4 (9h) BCLM (9h) and wtLCL23 (24h) cells. Bar=10μm.

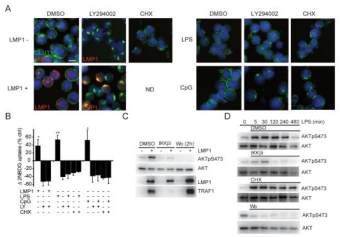

Figure 2. EBV LMP1-, LPS- and CpG- stimulated GLUT1 plasma membrane localization is dependent on AKT activation and continuous translation. AKT activation is both IKKβ and PI3K dependent

(A) GLUT1 localization (green), DNA staining (blue), and where indicated, LMP1 expression (red) in BL_{tet}LMP1 expressing LMP1 (24h), or stimulated with LPS (500ng/ml; 10h), or stimulated with CpG (250nM;10h). DMSO, LY294002 (LY;30μM) or CHX (10μg/ml) were included at 6h (LMP1) or 0h (LPS/CpG) where indicated. Bar=10μm. **(B)** Glucose/2NBDG import as in Figure 1A (n=3; mean±s.d., *p<0.05 /** p<0.005). **(C)** AKT activity in BL_{tet}LMP1 induced to express LMP1 and treated with DMSO, IKKβi (10μM at 6h) or Wortmannin (Wo;1μM at 22h). At 24h, total cell lysates were analyzed for LMP1, AKT and AKTpS473. TRAF1 serves as an indicator of NFκB activity. **(D)** AKT activity in uninduced BL_{tet}LMP1 pretreated with IKKβi, CHX or Wortmannin (Wo) for 15 min and then stimulated with LPS. Total cell lysates were prepared at the indicated times and analyzed for AKT and AKTpS473.

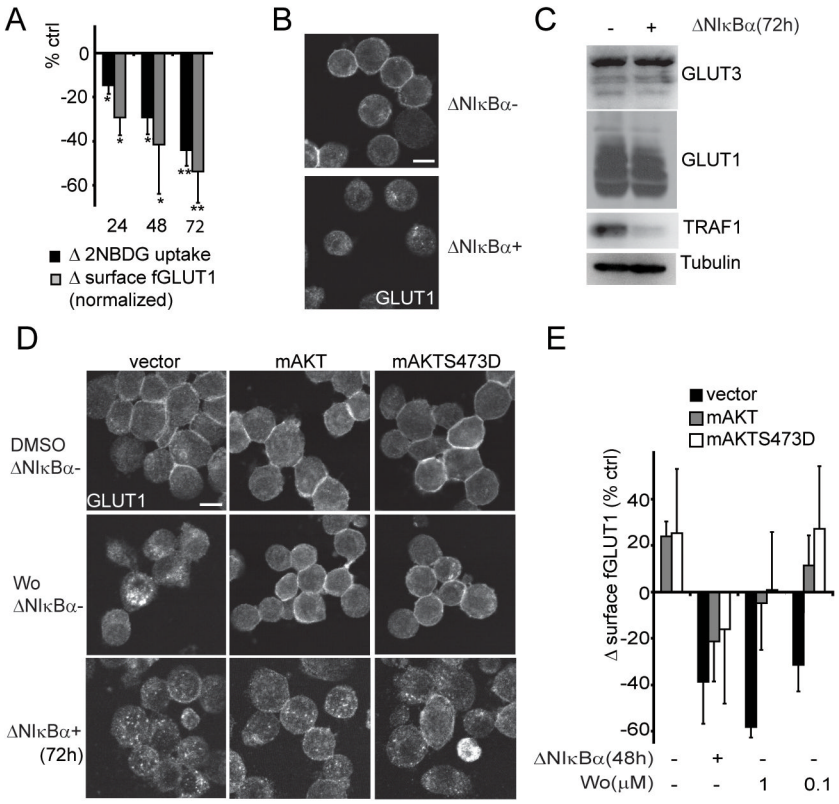

Figure 3. NFκB regulates GLUT1 localization downstream of AKT

(A) Glucose/2NBDG uptake (black bars) and surface fGLUT1 expression (grey bars) in IB4tetΔNIκBα and IB4tetΔNIκBα-fGLUT1 cells 24, 48 and 72h after ΔNIκBα induction. 2NBDG uptake was measured as in Figure 1A. Surface fGLUT1 signal was normalized to total fGLUT1 levels and presented as percent change over uninduced cells. Representative raw data found in Figures S3A and B. (n=3; mean±s.d., *p<0.05 /** p<0.005) **(B)** GLUT1 localization in $IB4_{tet}$ΔNIκBα with or without ΔNIκBα expression (72h). Bar=10μm. **(C)** GLUT1 and GLUT3 expression in total cell lysates from (B). TRAF1 expression is an indicator of NFκB activity, Tubulin a loading control **(D)** GLUT1 localization in Vector, myrAKT (mAKT) or myrAKTS473D (mAKTS473D) transfected $IB4_{tet}$ΔNIκBα after treatment with Wortmannin (Wo;9h) or induction for ΔNIκBα expression (72h). Bar=10μm. **(E)** Surface fGLUT1 in the indicated conditions 48h after transfection. $IB4_{tet}$ΔNIκBα-fGLUT1 cells were transfected with expression vectors for GFP and either control, myrAKT (mAKT) or myrAKTS473D (mAKTS473D). After 24h, ΔNIκBα was induced in one fourth of the cells. The residual uninduced cells were treated with either DMSO or Wortmanin (0.1 or 1μM) for the final 9h prior to determining surface fGLUT1 expression in GFP+ cells. Percent change over vector transfected, uninduced and untreated cells is presented. (n=3; mean±s.d., *p<0.05 /** p<0.005).

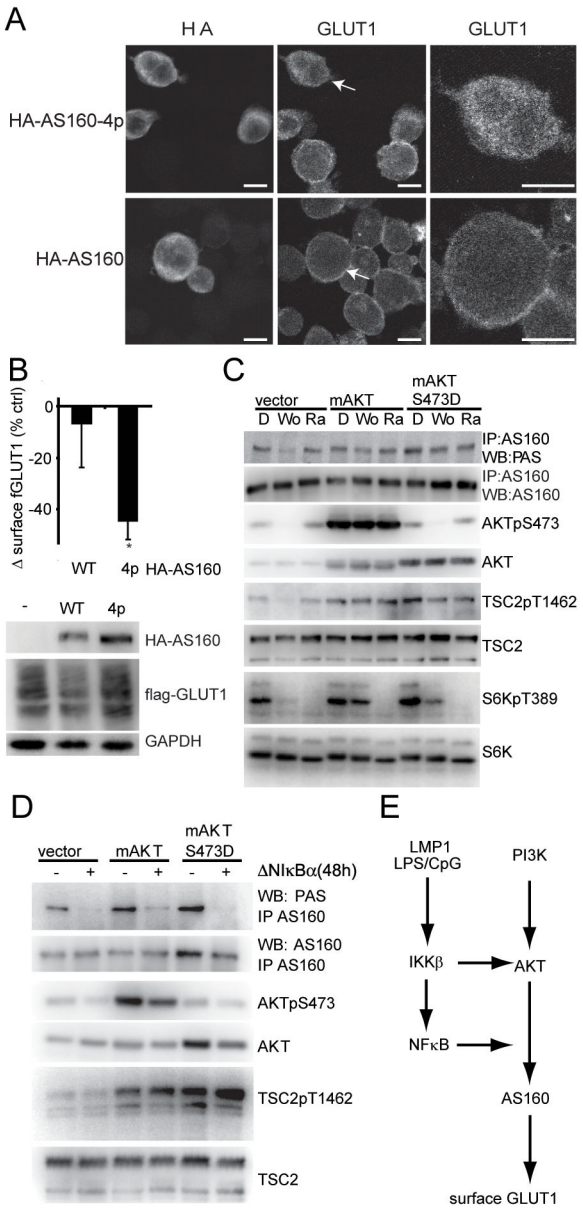

Figure 4. AKT-mediated phosphorylation of AS160 is dependent on NFκB transcription

(A) GLUT1 localization 24h after IB4 cells were transfected with wt HA-AS160 or mutant HA-AS160-4p, which can not be phosphorylated by AKT. Left panel, HA staining; Middle panel GLUT1 staining; right panel, GLUT1 staining, at higher magnification, of the indicated cell (white arrow) from the middle panel. Bar=10μm. **(B)** Surface fGLUT1 levels of GFP+ $IB4_{tet}$ΔNIκBα-fGLUT1 24h after transfection with expression vectors for GFP and either control vector, HA-AS160 or HA-AS160-4p. Percent change of surface fGLUT over control vector transfected cells is presented (n=4; mean±s.d. *$p<0.05$ /** $p<0.005$). Western blots of the corresponding total cell lysates analyzed for HA and flag. GAPDH served as a loading control. **(C)** AS160 phosphorylation at AKT substrate sites in vector, myrAKT (mAKT) or myrAKTS473D (mAKTS473D) expressing $IB4_{tet}$ΔNIκBα cells (uninduced) treated with DMSO (D), Wortmannin (Wo;1μM) or Rapamycin (Ra;500nM). At 9h, AS160 was immunopreciptiated and analyzed in Western blots for total AS160 expression and Pan

AKT Substrate (PAS) phosphorylation. Corresponding total cell lysates were analyzed for TSC2, TSC2pT1462, AKT, AKTpS473, S6K and S6KpT389. Note myrAKTS473D is not detected by the AKTpS473 antibody **(D)** AS160 phosphorylation at AKT substrate sites in vector, myrAKT (mAKT) or myrAKTS473D (mAKTS473D) expressing $IB4_{tet}$ΔNIκBα cells either uninduced (−) or induced (+) to express ΔNIκBα for 48h. AS160 was immunoprecipitated and analyzed for total AS160 PAS phosphorylation. Corresponding total cell lysates were analyzed in Western blots for TSC2, TSC2pT1462, AKT and AKTpS473 **(E)** Model depicting the dual role of the NFκB pathway in regulating AKT and GLUT1.

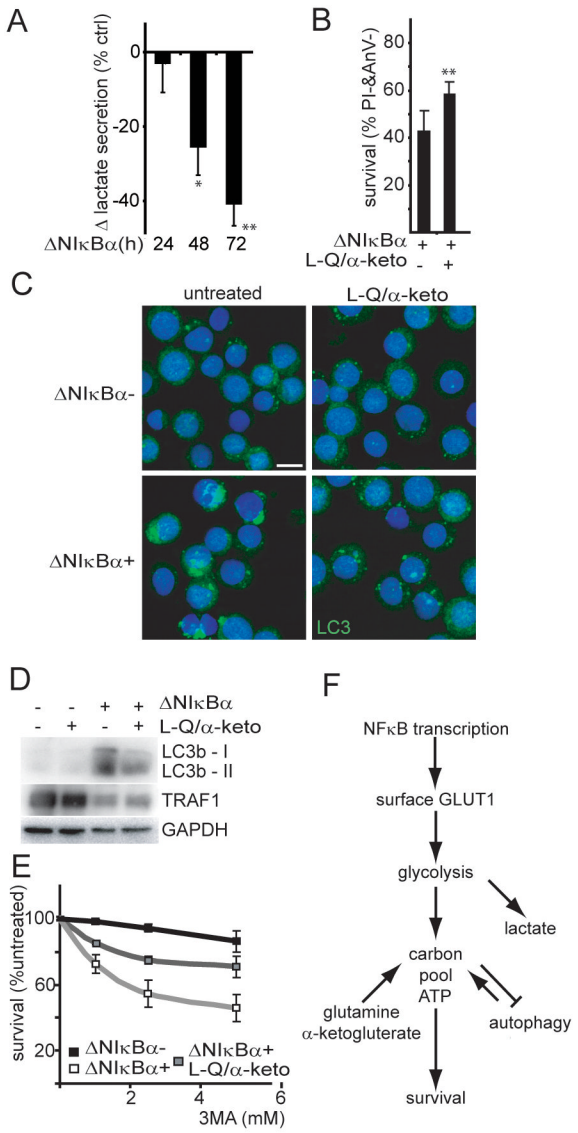

Figure 5. NFκB-mediated transcription links carbon availability to cell survival in a model of NFκB dependent lymphoma

(A) Rate of lactate production of IB4$_{tet}$ΔNIκBα expressing ΔNIκBα at indicated time points. The percent change over uninduced cells is presented (n=3; mean±s.d. *p<0.05 /** p<0.005). **(B)** Cell survival (% Annexin V^{-}, Propidium Iodide^{-}) of ΔNIκBα expressing cells grown in normal media with or without supplemental Glutamine (L-Q;22mM) and α-ketoglutarate (α–keto;20mM), (day 5, n=8; mean+s.d., **p<0.005). **(C)** Autophagosome marker LC3b localization (green) and DNA (blue) in ΔNIκBα- and ΔNIκBα+ IB4$_{tet}$ΔNIκBα grown with QVD (10uM) with or without supplemental glutamine and α-ketoglutarate (72h). Bar=10μm. **(D)** Whole cell lysates corresponding to (C) were analyzed for LC3b-I and autophagosome associated LC3b-II expression. TRAF1 and GAPDH served as controls for NFκB activity and loading respectively. **(E)** Cell survival (high forward scatter, low side scatter) after autophagy inhibition with 3-methyladenine (3MA). IB4$_{tet}$ΔNIκBα were cultured ΔNIκBα-(black),ΔNIκBα+ (white), or ΔNIκBα+ with supplemental glutamine and α-ketoglutarate (grey). After 48h the indicated concentrations of 3MA were added for an additional 18–24h. Percent cell survival was normalized to non 3MA treated cells (n=3;

mean±s.d.); ΔNIκBα-= 89%; ΔNIκBα+ = 69%; ΔNIκBα+ & L-Q/α-keto= 81%. **(F)** Model: Impact of NFκB transcription on metabolism.